MATHEMATICAL MODELING OF CANCER CELL GROWTH IN THE PRESENCE OF CYTOTOXIC DRUGS

by

Madison Frieler

Submitted in partial fulfillment of the
requirements for Departmental Honors in
the Department of Biology
Texas Christian University
Fort Worth, Texas

May 4, 2020

MATHEMATICAL MODELING OF CANCER CELL GROWTH IN THE PRESENCE OF CYTOTOXIC DRUGS

Project Approved:

Supervising Professor: Giridhar Akkaraju, Ph.D.

Department of Biology

Hana Dobrovolny, Ph.D.

Department of Physics and Astronomy

Molli Crenshaw, MS

Department of Biology

Abstract

Cancer has one of the biggest impacts on our society as almost 2 million new cases will be diagnosed each year and approximately 38% of people in the US will be diagnosed with cancer at some point in their life. Cancer is the uncontrolled proliferation of cells in the body due to mutations that result in tumors. Current systems that model the growth of cancer cells by determining the IC_{50} are inefficient because they are time dependent and often do not consider the E_{max} value, leading to inconsistencies in the IC_{50} value obtained. The IC_{50} value is important in consistently giving the correct dosage of chemotherapy drugs to patients. Another common issue with chemotherapy drugs is the side effects caused by high dosages and nonspecific cellular targets. These effects can significantly impact a patient's quality of life and cause other significant health problems after the chemotherapy. The use of nanoparticles to deliver anticancer drugs to cancer cells may improve the side effects often associated with chemotherapy by targeting cancer cells with greater specificity and killing smaller amounts of noncancer cells. Carbon allotropes such as carbon nanotubes (CNTs) and nitrogen doped graphene quantum dots (NGQDs) can be linked to chemotherapy drugs to better target cancer cells because they possess qualities such as resistance to degradation, increased circulation time, and high surface area to volume ratio. Our project aims to create a new mathematical model which is time independent to provide a better, more consistent IC_{50} value to use in the dosage of drug. In addition, we are exploring the use of carbon nanoparticles in targeting cancer cells and their ability to decrease the amount of drug necessary therefore decreasing the IC_{50} of the drug, resulting in decreased chemotherapy side effects.

Introduction

Cancer is the second leading cause of death in the United States. The incidence of cancer in the United States is 439.2 per every 100,000 people and 163.5 for every 100,000 per year died due to cancer from 2011 to 2015 (1). Specifically, breast cancer is the second most common cancer in women and rates of breast cancer are expected to continue to rise in the future (1). Cancer is a disease of pathological hyperplasia of cells due to mutations that allow traits such as self-sufficient growth signals, evasion of apoptosis, and sustained angiogenesis (2). One of the most common methods of treating cancer is chemotherapy. Many chemotherapies work by damaging DNA in cancer cells. For example, platinum-based chemotherapies work by using alkylating agents to form covalent linkages in macromolecules. These alkylating agents form covalent bonds in DNA between adenines or guanines via the platinum atom which causes interstrand and/or intrastrand crosslinks (Figure 1.) (3). These crosslinks result in inhibition of DNA replication.

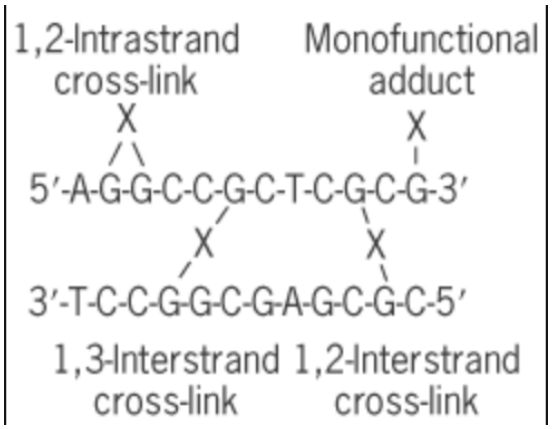

Figure 1. 1,2- and 1,3-interstrand and intra strand cross link induced by antitumor agents (3).

The anticancer drug doxorubicin is a commonly used treatment that also damages cell DNA by disrupting topoisomerase-II (TOP2)-mediated DNA repair and generating free radicals to disrupt the cell membrane (Figure 2.) (4).

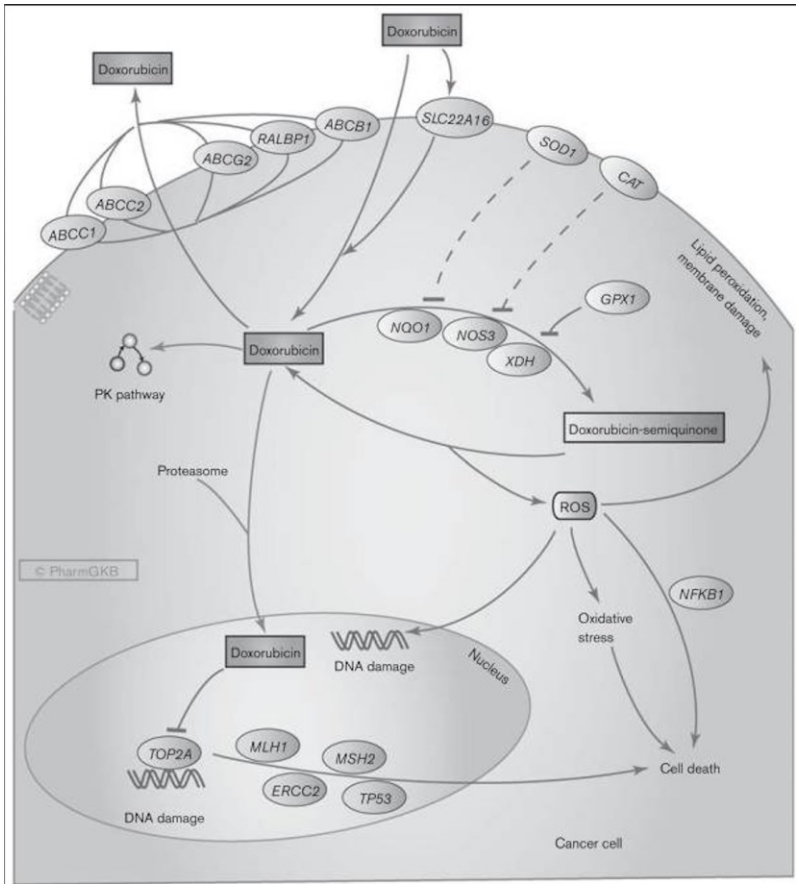

Figure 2. Mechanism of doxorubicin (4).

The replication of DNA and the transcription of RNA results in supercoiling of DNA strands. TOP2a and TOP2b create paired DNA strand breaks. The critical intermediate for this reaction is the TOP2 cleavage complex. Topoisomerase II inhibitors such as doxorubicin stabilize this complex which leads to an accumulation of double stranded breaks because relegation is

inhibited. This results in accumulation of DNA damage which will lead to cell death in rapidly dividing cells (Figure 3)(5).

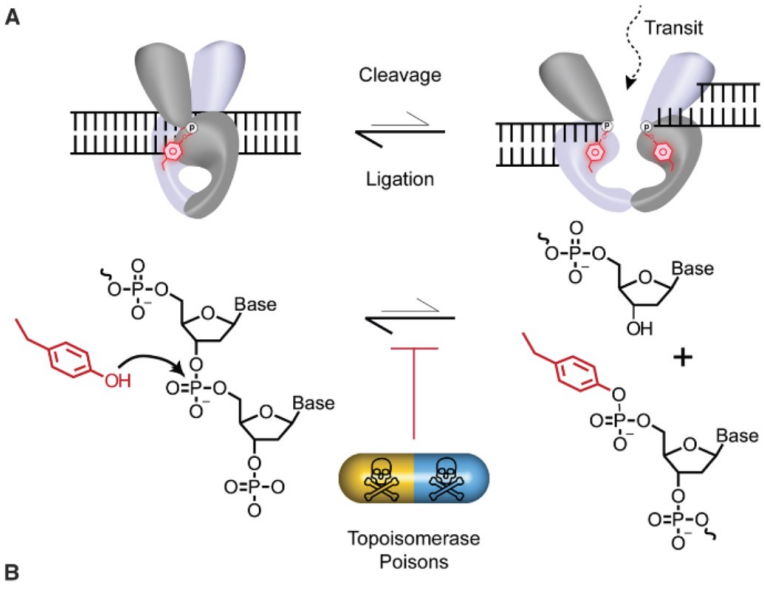

Figure 3. Topoisomerase-2 cleavage ligation equilibrium and topoisomerase poisons (5)

One problem with many current chemotherapies including platinum-based drugs and doxorubicin is their lack of ability to differentiate between normal cells and cancer cells. These drugs will target any dividing cell. While drugs such as doxorubicin may kill cancer cells at a higher rate because they are dividing more rapidly, there are still many side effects associated with these drugs. One important side effect of doxorubicin is cardiovascular toxicity which can lead to hypotension, tachycardia, arrythmias, and congestive heart failure (6). The incidence of doxorubicin cardiomyopathy can be as high as 36% when a person's lifetime dose exceeds 600mg/m^2 (6). Experiments have shown that doxorubicin can accumulate in the mitochondria which could explain why doxorubicin can be toxic for cardiac cells (6). The toxicity may be due to an accumulation of iron in the mitochondria, contributing to oxidative stress in the cell. The drug could also contribute to opening of the mitochondrial permeability transition pore opening

which inhibits the ability of the inner membrane of the mitochondria to maintain an electrochemical gradient (6). Nanoparticle delivery can decrease toxicity of chemotherapy drugs by decreasing the dose necessary to effectively kill cancer cells. Since many side effects of these drugs are dose-dependent, these side effects could be minimized through the use of nanomaterials as a delivery method. Nanoparticles also have the potential to increase efficiency of delivery by attaching targeting agents such as hyaluronic acid. The fluorescent properties of nanoparticles also offer the possibility to track chemotherapy delivery in cells and tissues. The strong fluorescence, due to quantum confinement and edge effects, could allow monitoring of the activity of the drug and its release into the tissues in real time (1). A variety of different nanoparticles, characterized as being less than 100nm, are being tested in cancer research, some of which include quantum dots, carbon nanotubes, silicon nanomaterial, gold nanoparticles, silver nanoparticles, and superparamagnetic nanoparticles (7). Gold nanoparticles are being tested for use in early detection of certain cancers. Researchers looked at the ability of the gold particles to distinguish cancer cells from noncancer cells by detecting the epidermal growth factor receptor, which is overexpressed in many epithelial cancers (8). The gold nanoparticles allow for optical contrast and enhanced Raman scattering to detect epithelial cancers, such as oral cancer, earlier (8).

Current research is looking at carbon allotropes as a method of drug delivery because of the unique qualities they possess. Specifically, carbon nanotubes (CNTs) allow for attachment of a high density of drug because of their high surface area to volume ratio, their ability to attach to targeting agents, their evasion of the immune system when equipped with targeting agents(9). Quantum dots also offer many unique properties such as biocompatibility, solubility in water, prolonged circulation time in the body, and are resilience against degradation (10). These

properties give carbon nanomaterials a variety of applications in medicine. CNTs, which have a large surface to recognize and display elements, have been studied for use as biosensors to sense substances such as DNA, glucose, and cancer biomarkers (11). CNTs may also be used for regenerative medicine to improve bone regeneration and artificial tissue scaffolding (11). Another type of carbon nanomaterial that may be used are graphene-based substances used in photothermal therapy to treat cancer. Graphene materials are able to interact with low frequency photons at infrared frequencies and generate heat plasmonic photothermal conversion (11).

While nanoparticles may offer many benefits to drug delivery, imaging, and biosensing, there are also possible complications of using nanomaterials in humans. One risk is the possibility that the nanoparticles could aggregate and be toxic to vital organs. This could result in the formation of harmful metabolites and damage to these organs (12). Silver nanoparticles have been shown to accumulate in lungs, spleen, liver, kidneys, and brain after rats either inhaled or were injected subcutaneously with the particles (12). Accumulation could lead to increased generation of reactive oxygen species in these organs (12). Additionally, CNTs have been shown to cause pulmonary fibrotic lesions similar to those of idiopathic pulmonary fibrosis (13). One possible mechanism for this fibrosis is activation of Th2-type cytokines after exposure to CNTs, specifically, IL-4 and IL-13, which are associated with fibrosis, was shown to increase in response to single walled CNTs (13). These possible complications of nanomaterials require further in vivo studies to determine the cytotoxic effects of these particles.

Quantum dots have been shown to be a promising tool to deliver drugs to cancer cells because of their ability to be taken up by the cell and the ability to track the quantum dots because of their fluorescent properties. QDs also show increased biocompatibility compared to other nanoparticles. When imaged in cell culture over 32 hours, QDs showed decreased size and

degradation at 24 hours and by 32 hours they appear to be partially to fully degraded (14). The time-dependent degradation seen in QDs is unique and offers decrease risk of accumulation toxicity to cells compared to other nanomaterials. In previous studies graphene quantum dots have been incubated with MCF-7 cells and shown to localize in the late-stage endosome and lysosome indicating the material is taken up via endocytosis (1). Graphene quantum dots were also shown to be taken up by precision cut mammary tumor slices without obvious negative effects (1). These studies indicate these nanoparticles as a possible new tool for drug deliver to cancer cells (1).

While nanoparticles offer excellent possibility for more efficient drug delivery, modeling of tumor growth of cancer cells treated with nanoparticle delivered chemotherapy does not exist. Modeling the growth of cells after treatment with these materials poses significant challenges because of the wide range of different nanoparticles being studied. Analyzing growth of cancer cells is important in giving the correct chemotherapy drug dosage to patients. Current strategies use the IC_{50} and less commonly the E_{max} to give the correct dosage of drug to a patient. The IC_{50} is the concentration of drug where the cell count is half the control and the E_{max} is the number of viable cells at the highest drug concentration (15). Current models of cell growth are time-dependent and are considered static. Often the Hill equation is used and a "sigmoidal dose–response curve that summarizes the relationship between drug effect and concentration" (16). The time-dependent nature of these curves can lead to inaccuracies because these models are biased towards exponential growth and delays in drug effect stabilization (16). In this work based on experimental *in vitro* studies with nanomaterials-delivered chemotherapy and chemotherapy drug alone we propose a method of cancer cell growth modeling that will include an E_{max} value, which is often not characterized and, most importantly, is time-independent. This

will allow more consistent assessment of the efficiency of anti-cancer drugs and nanomaterials-delivered formulations.

The development of a new, time independent model for determining the IC_{50} and E_{max} of a drug will allow a more consistent measurement of the efficiency of these drugs and the efficiency will be further improved with the addition of delivery via nanomaterial.

Methods

Cell Culture

MCF-7, HEK293, and HeLa cells were grown in cell culture using Dulbecco's modified eagle media (DMEM, 10% fetal bovine serum, 1% non-essential amino acids, L-glutamine, Penicillin, Streptomycin) at 37°C and 5% CO_2. When cells reached confluency the medium was aspirated, cells were washed with 1x PBS. 0.05% trypsin was added to detach cells and was then quenched with DMEM. Cells were then counted using a hemocytometer and plated for use in an experiment and 10% of cells are added to a new flask with DMEM.

Cell Growth Assay

MCF-7, HEK293, and HeLa cells were plated on 12 well trays at a density of 500, 1,000, or 2,000 cells/well with 2 mL of medium in each well, depending on the experiment. The plates were incubated at 37°C and 5% CO_2. After 24 hours drug was added as indicated. After another 24 hours medium was removed from 3 of the wells and washed with 1x PBS. 0.05% trypsin was added to detach the cells and medium was added to quench the trypsin. Cells were then counted using a hemocytometer and steps were repeated for each concentration of drug, if necessary.

Synthesis of Dox-PEG-CNT

Dox, CNT, and polyethylene glycol (PEG) were mixed in a ratio of 0.59 mg Dox: 0.2 mg CNT: 0.5 PEG: 1ml water. This solution was sonicated in a Covaris bath sonicator for 32 cycles of 30 second bursts. This allowed the nanotubes to disperse and allowed non-covalent bonds to form between Dox, PEG, and CNT. The solution was then filtered through a 100kDa centrifuge filter at 1200 g and washed three times with water in order to remove excess Dox and PEG.

MTT Cell Viability Assay

Cells were plated at a density of 5,000 cells/well on a 96 well tray and incubated at 37ºC and 5% CO_2. After 24 hours the cells were treated with increasing concentrations of doxorubicin, Dox-PEG-CNT, or Dox-QD. The cells were treated with drug for 16 hours and then the medium was removed from the wells. A solution of 1mg/ml thiazolyl blue tetrazolium bromide (MTT) in serum free medium was made and 100 µL was added to each well and incubated at 37ºC for 4 hours. Then the MTT solution was removed and 100 µL of dimethyl sulfide (DMSO) was added. Cells were then placed on a shaker for 5 minutes and the absorbance was measured at 540nm.

Synthesis of Dox-QD

A solution of Dox-QD was made by combining 1 mL of Dox at a concentration of 0.0041mg/mL and added to 41mg of nitrogen doped quantum dots (NGQDs). This solution was sonicated in a Covaris bath sonicator for 7 cycles of 30 second bursts.

Results

First, in order to measure the effect of chemotherapy drugs and the growth rate of cells, we determined a baseline of cell growth. To do this we tested the rate of growth of three different cell types; HeLa cells, a cervical cancer cell line, MCF-7, a breast cancer cell line, and HEK293 cells, human embryonic kidney cells obtained by transforming primary cells with Adenovirus DNA. Each cell type was grown over a period of 14 days and counted every other day. Figure 2 shows the growth curve obtained for each cell type. HeLa and HEK293 cell growth peaked at day 10, while MCF-7 cell growth peaked on day 12. The subsequent decline seen is due to overcrowding of the wells and a buildup of waste in the medium. Having established a baseline for cell growth, we the tested the cytotoxic effect of doxorubicin, an anticancer drug, on cell growth. After treatment we measured the percent of surviving cells and calculated a coefficient of determination (R^2) value of 0.712 for HEK293 cells, 0.955 for MCF-7 cells, and 0.983 for HeLa cells (Figure 3). This value indicates the proportion of variance in cell survival which can be predicted by doxorubicin toxicity. Then, we examined how doxorubicin affected the growth of each cell line. For HEK293, HeLa, and MCF-7 cells we added doxorubicin at the indicated concentrations following which the rate of growth was determined for HEK293, HeLa cells, and MCF-7 cells (Figs. 4a, 4b and 4c, respectively). The highest concentration of doxorubicin used (0.05 μg/mL) proved to be too toxic to the cells, resulting in no measurable cell growth in all cell lines tested. In HEK293 cells all concentrations other than 0.05 μg/mL showed a similar rate of growth, including the cells which had no drug added. HeLa cells showed varying growth rates per concentration, and MCF-7 cells showed a decreased growth rate as concentration of doxorubicin increased.

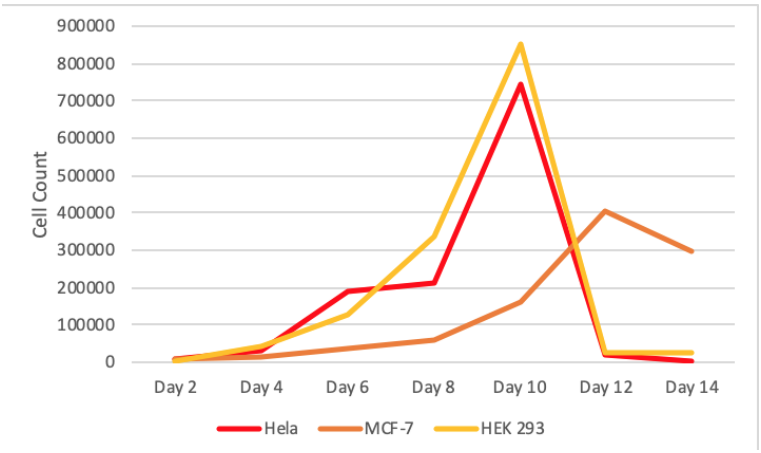

Figure 4. Growth of HeLa, MCF-7, and HEK293 cells over 14 days.

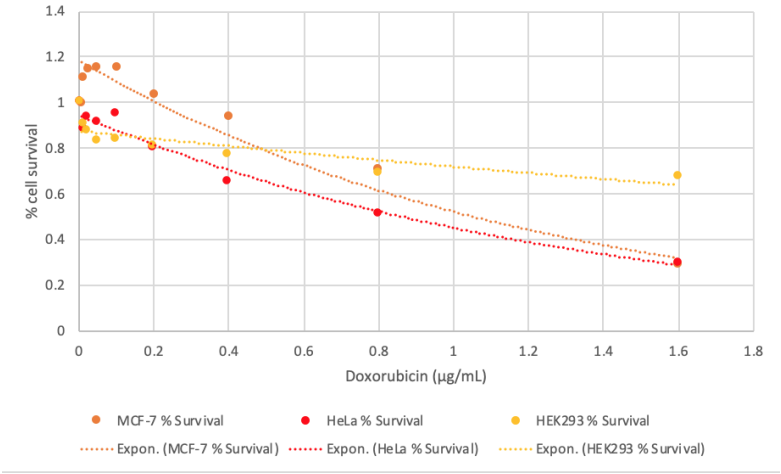

Figure 5. Cytotoxicity of doxorubicin on MCF-7, HeLa, HEK 293.

a

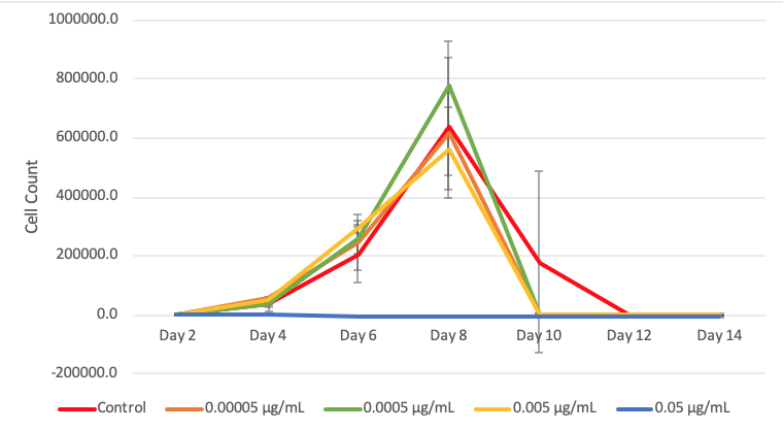

b

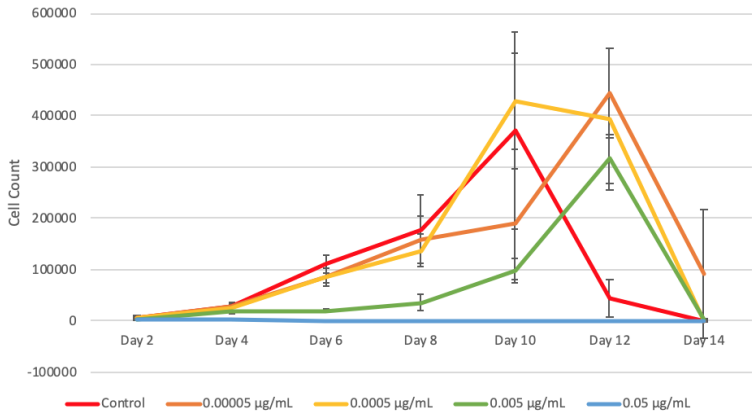

c

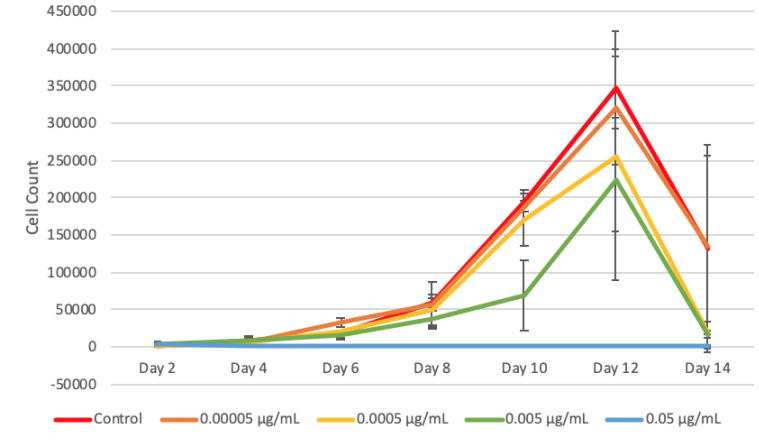

Figure 6. (a) HEK 293 growth curve after treatment with doxorubicin. (b) HeLa growth curve after treatment with doxorubicin. (c) MCF-7 growth curve after treatment with doxorubicin.

The cell growth rate data obtained was used to model the growth of the cells following treatment with the chemotherapy drug, in a time independent manner (figure 5). A logistic model was used, given by the equation:

$$\frac{\mathrm{d}N}{\mathrm{d}t} = \lambda N \left(1 - \frac{N}{K}\right),$$

Where N is the number of cancer cells, λ is the growth rate, and K is the carrying capacity. NGQD have been shown to bind to doxorubicin with a high affinity, and to have favorable dissociation kinetics, an essential requirement for delivery of the agent to the target cells. (12) After modeling the growth rate of cells with doxorubicin we evaluated the efficiency of NGQD-mediated delivery of doxorubicin to cells. However, we first needed to test toxicity of NGQD, NGQD with doxorubicin (NGQD/Dox), and doxorubicin on MCF-7 cells to compare survival of cells when NGQD/Dox vs. doxorubicin was added. In order to determine that any decrease in survival rate is attributed to doxorubicin, we looked at the rate of survival with only NGQDs. First, we assessed the cytotoxicity of NGQD, NGQD/Dox, and doxorubicin on MCF-7 cells using a colorimetric assay with established dye 3-(4,5-dimethylthiazol-2-yl)-2,5-diphenyltetrazolium bromide (MTT). MTT stains living cells allowing us to calculate percent cell survival as a function of treatment (figure 6). NGQD alone showed very little toxicity to cells. NGQD/Dox was more cytotoxic to cells than cells treated with Doxorubicin alone.

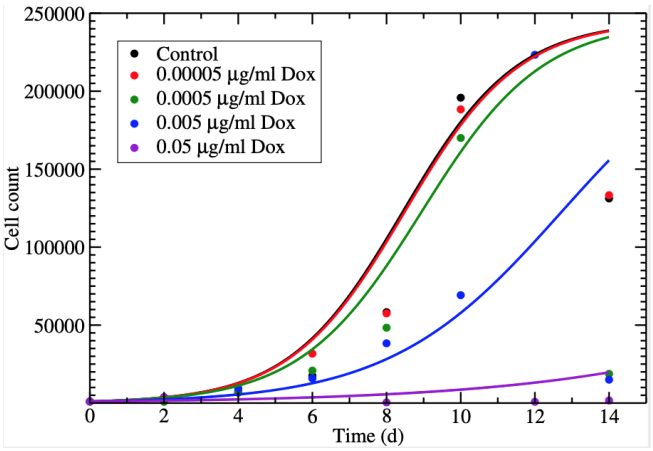

Figure 7. Mathematical model fit to growth data of MCF-7 treated with Dox.

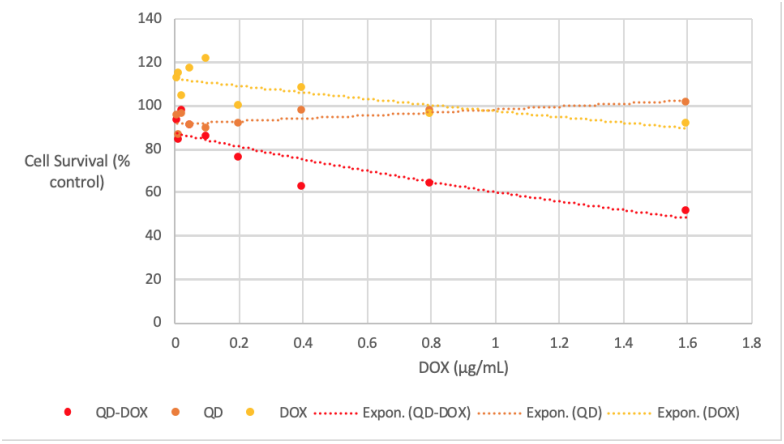

Figure 8. Cytotoxicity of doxorubicin NGQD/Dox, and NGQDs on MCF-7.

Next, we wondered how the NGQD/doxorubicin conjugate would affect the rate of growth of MCF-7 cells. This would allow comparison of the growth curves of NGQD/Dox to only doxorubicin treatment. MCF-7 cells were treated with the NGQD/Dox at the indicated concentration and counted every other day for 14 days (figure 7a). At concentrations of 0.005 µg/mL and 0.05 µg/mL cells treated with NGQD/Dox showed no cell growth indicating that these concentrations were too toxic. The growth of MCF-7 cells after treatment with NGQD/Dox was modelled using the same equation as shown above (Figure 7b). A comparison of the IC_{50} and E_{max} in cells treated with doxorubicin alone vs. cells treated with varying concentrations of

NGQD/Dox is shown in Table 1. A decrease in the IC_{50} and an increase in the E_{max} can be seen with the NGQD/Dox conjugate compared to doxorubicin alone.

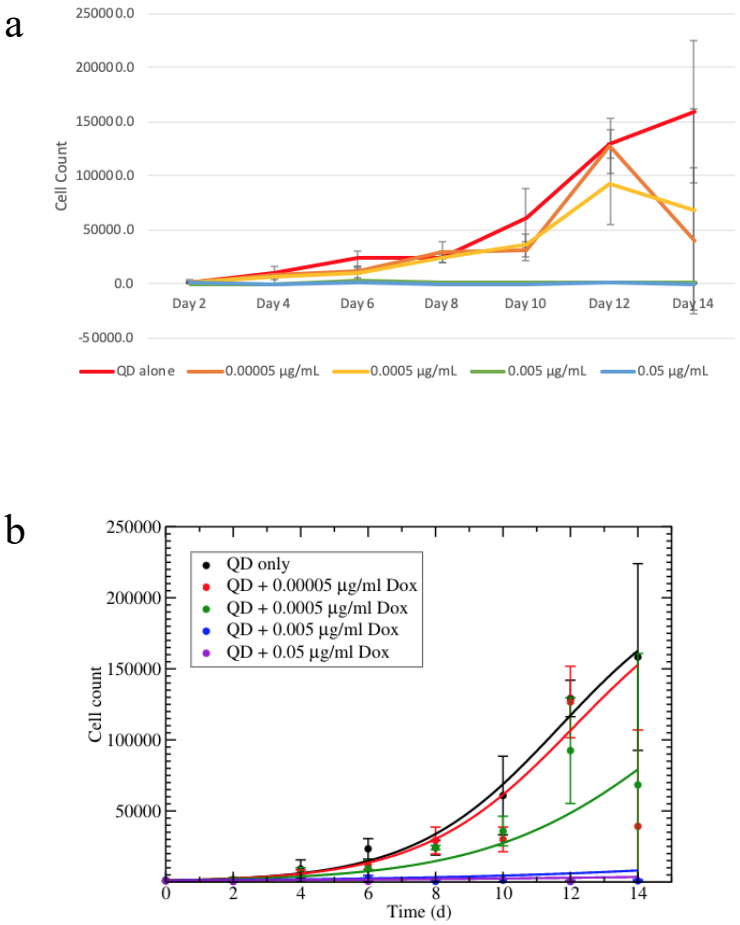

Figure 9. (a) MCF-7 growth curve after treatment with NGQD/Dox treatment. (b) Mathematical model fit to growth data of MCF-7 treated with NGQD/Dox.

Parameter	λ (/d)	K (cells)
DOX alone	0.652 (0.492–0.964)	2.45×10^{5} $(1.51–4.66)\times10^{5}$
QD + DOX	0.460 (0.433–0.488)	2.19×10^{5} $(1.82–2.73)\times10^{5}$
Parameter	IC_{50} (µg/mL)	ε_{max}
DOX alone	6.06×10^{-3} $(0.937–29.7)\times10^{-3}$	0.745 (0.359–1.00)
QD + DOX	1.12×10^{-3} $(0.307–4.60)\times10^{-3}$	0.820 (0.387–1.00)

Table 1. Best fit parameters with 95% confidence interval for MCF-7 growth.

Measurement of cell growth based on cell count can be a subjective endeavor prone to observer error. To eliminate this, a different method (MTT assay) was used to measure cell survival to measure growth rate of MCF-7 cells in the presence of doxorubicin and NGQD/Dox. Doxorubicin (figure 8a) or NGQD/Dox (figure 8b) was added to cells at the indicated concentrations and cell survival measured on days 2,4,6, and 8. These studies showed a steady increase in cell growth rate for both treatments over the 8-day period. The IC_{50} for the two treatments was determined using the data obtained (Fig. 9). The IC_{50} value for NGQD/Dox was lower than doxorubicin alone. These results were similar to those seen when the IC_{50} values were calculated using the mathematical models of cell growth.

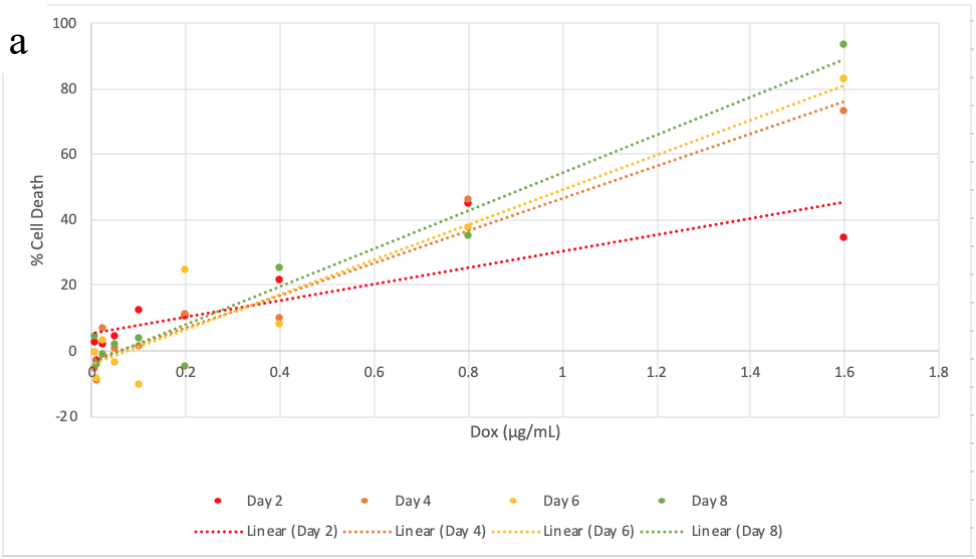

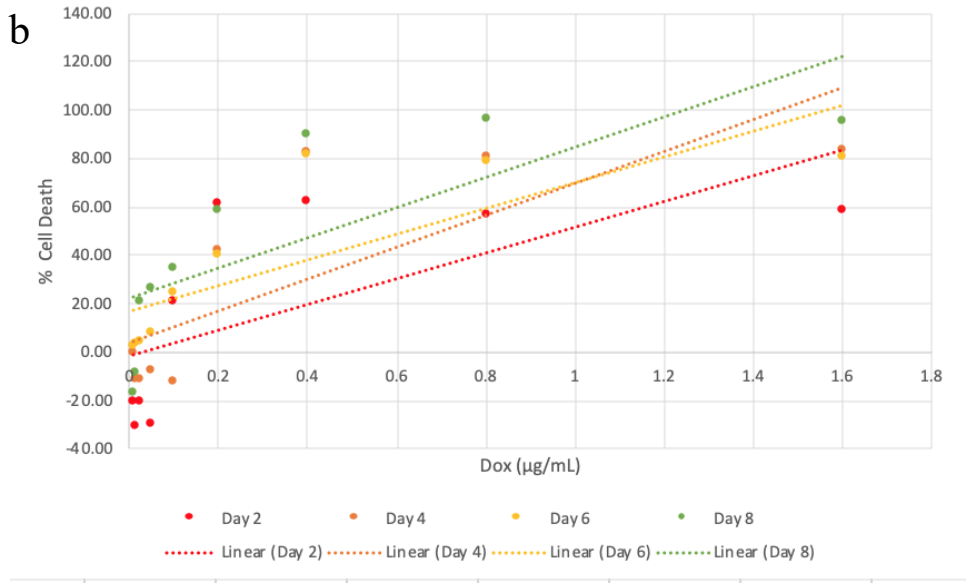

Figure 10. (a) Rate of MCF-7 cell death after doxorubicin treatment. (b) Rate of MCF-7 cell death after NGQD/Dox treatment.

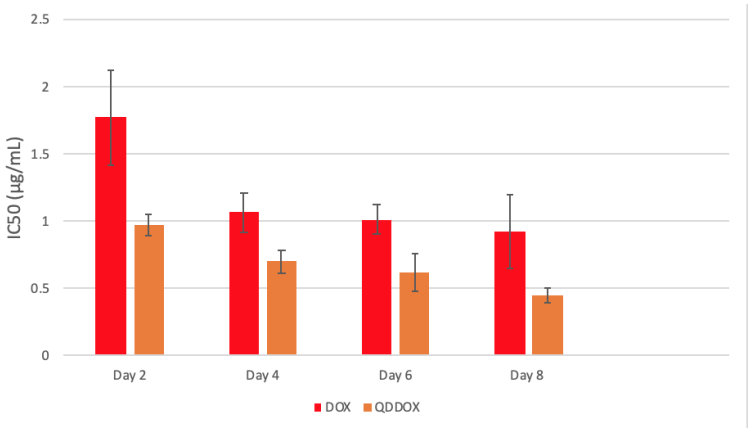

Figure 11. IC_{50} of doxorubicin on MCF-7; IC_{50} of NGQD/Dox on MCF-7.

To localize the drug and to determine the rate of drug loss from the target cells, they were visualized using three-dimensional confocal fluorescent imaging. Figure 10 a-f shows the fluorescence of doxorubicin in the cells at the timepoints indicated. The images indicate that doxorubicin localized primarily in the nucleus. Next, the efficiency of internalization of NGQD/Dox was determined. Cells were imaged using fluorescence and the corrected total cell fluorescence for each time point (3, 6, 9, 12, and 24 hours) was calculated and is shown in figure 10g. The internalization of doxorubicin into cells is the highest 9 hours after treatment and the level of drug stays consistently high in the cells for up to 24 hours post treatment.

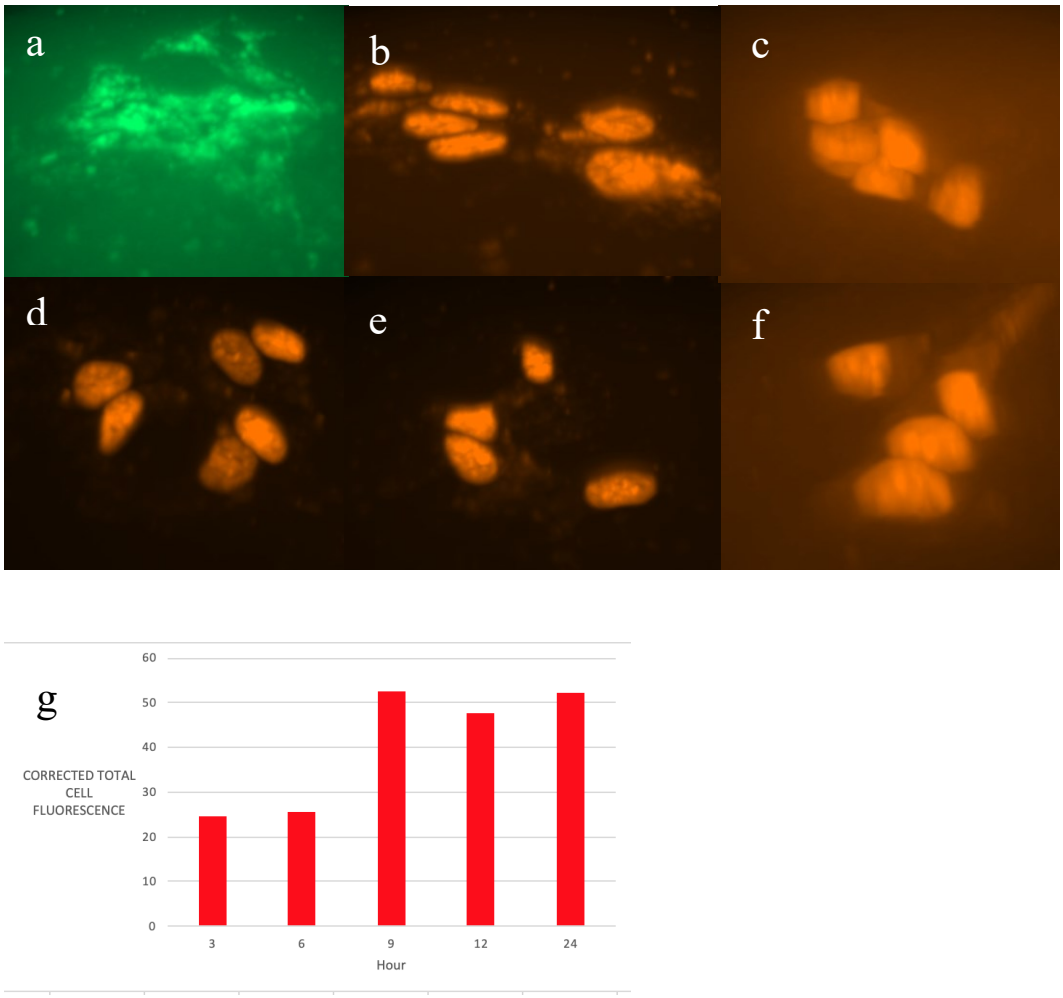

Figure 12. (a) Three-dimensional confocal fluorescent imaging of MCF-7 with NGQDs for 3 hr. (b) with NGQD/Dox for 3 hr. (c) with NGQD/Dox for 6 hr. (d) with NGQD/Dox for 9 hr. (e) with NGQD/Dox for 12 hr. (f) with NGQD/Dox for 24 hr. (g) Corrected total cell fluorescence of doxorubicin in MCF-7 by hour.

Discussion

Previous studies have shown the biocompatibility, prolonged circulation time in the body, and water solubility of nanomaterials, making them well suited to be agents for the delivery of chemotherapy drugs. Specifically, NGQDs have been shown to have a high affinity for the common anti-cancer drug, doxorubicin. These nanoparticles offer the benefit of a possible reduction in the harmful side effects of chemotherapy because of reduction in the dose necessary to treat the cancer. In addition, consistently finding the correct dose of chemotherapy to treat patients is vital to killing the cancer while saving as many non-cancer cells as possible to reduce damage to these healthy cells. Currently, mathematical modeling of the growth rate of cancer cells is time dependent and often does not consider the E_{max} value. The time-dependent nature of tumors makes this modeling inconsistent. Furthermore, there is not a model available to model growth when chemotherapy is combined with nanoparticles. Creating a model which is time-independent, considers the E_{max}, and can account for nanoparticle-based drug delivery, would allow for more accurate dosing and delivery of chemotherapeutic agents to patients. Reducing side effects of commonly used chemotherapies is essential in improving quality of life and increasing life expectancy for cancer patients.

First, we established a baseline of cell growth for all cell lines and found HeLa and HEK293 cell growth peaked at day 10 while MCF-7 growth peaked at day 12. This data was used to compare against cells grown in the presence of chemotherapy. Next, we found the percentage of cell survival after treatment with doxorubicin. Our results indicate that MCF-7 and HeLa cells died at a higher rate than HEK293 cells, which may be due to the way each cell line was made. HEK293 cells were transformed using Adenovirus DNA while HeLa and MCF-7 were isolated from cancer cells. This may be due to the transformation process using Adenovirus

DNA to make HEK293 cells as opposed to HeLa and MCF-7, which originate from cancer cells. When growth of each cell line was measured in the presence of increasing concentrations of doxorubicin, all three cell lines showed no cell growth at any concentration above 0.05 μg/mL. We concluded that this concentration was too toxic for growth. In HEK293 and HeLa cells, concentrations below 0.05 μg/mL of doxorubicin showed no statistically significant difference in cell growth. However, MCF-7 cells showed decreasing growth as the drug concentration increased, indicating a dose-dependent response in these cells. Therefore, we used the MCF-7 cell line to mathematically model the growth of cells in the presence of doxorubicin. Mathematically modeling the growth of these cells showed growth curves similar to those obtained by manually counting the cells. This indicates that the model is able to accurately represent the growth rate of MCF-7 cells after they are treated with doxorubicin.

Next, we measured the cytotoxicity of NGQDs and NGQD/Dox on MCF-7 cells. NGQD alone showed almost no toxicity to the cells, while the conjugate was more toxic to the cells than doxorubicin alone. Therefore, when doxorubicin is conjugated to NGQDs it is able to kill MCF-7 cells more efficiently than unconjugated doxorubicin. When MCF-7 cells were grown and counted for 14 days after treatment with the NGQD/Dox, the highest concentrations, 0.005 μg/mL and 0.05 μg/mL killed all cells. In comparison, when doxorubicin alone was added to the cells at a concentration of 0.005 μg/mL, less cell death was observed. This result supports the conclusion that the conjugate is more toxic to cancer cells than doxorubicin alone. Modeling of cells after they were treated with NGQD/Dox was also able accurately display the growth of MCF-7 cells, using the same method as was used for doxorubicin alone. When IC_{50} and E_{max} of both doxorubicin and the NGQD/Dox were compared, the conjugate showed a decreased IC_{50} and an increased E_{max}. A decreased IC_{50} indicates that a smaller concentration of the conjugate is

able to inhibit 50% of the cells, which is beneficial because a smaller amount of drug can be used to kill the cancer cells resulting in less side effects. Additionally, an increased E_{max} supports the results which indicate the conjugate is more toxic to MCF-7 cells than only doxorubicin.

When an alternative method, measuring cell survival to assess cell growth, was used, a steady rate of growth over 8 days was seen in MCF-7 cells after doxorubicin or NGQD/Dox was added. IC_{50} calculations using this data showed a decreased IC_{50} for the conjugate compared to cells treated with doxorubicin alone. These results confirm the conclusions found using the primary method, cell counting in conjunction with mathematical modeling, which indicated a decreased IC_{50} when using the conjugate.

Confocal imaging of MCF-7 cells after treatment with NGQD/Dox showed localization of doxorubicin mainly in the cell nucleus. This finding supports the proposed mechanism of action of doxorubicin, because the target of this drug, a topoisomerase II inhibitor, involved in DNA replication, is present in the cell nucleus. A time course experiment, measuring the efficiency of internalization of doxorubicin into the cells indicated that internalization was highest 9 hours after treatment with the conjugate and this level of internalization was maintained up to 24 hours following treatment. These results indicate that the conjugate remains in the cells for at least 24 hours following treatment, allowing the drug to efficiently kill the cell.

Our results support the hypothesis that a conjugation of NGQDs with doxorubicin is more toxic to the cells than doxorubicin alone. This may allow for a decrease in required dose of drug needed to kill cancer cells in the body, resulting in reduced side effects. In addition, we have provided a mathematical model of this cell growth, which can accurately portray the rate of cancer cell growth after treatment with doxorubicin or NGQD/Dox in a time-independent matter. The combination of these findings will allow for more consistent measurements of the

effectiveness of chemotherapy drugs and the possibility of lower dosages which would decrease the risk of side effects which result from high doses of chemotherapy.

References

1. Kersting, D.; Fasbender, S.; Pilch, R.; Kurth, J.; Franken, A.; Ludescher, M.; Naskou, J.; Hallenberger, A.; Gall, C. v.; Mohr, C. J.; Lukowski, R.; Raba, K.; Jaschinski, S.; Esposito, I.; Fischer, J. C.; Fehm, T.; Niederacher, D.; Neubauer, H.; Heinzel, T. From in vitro to ex vivo: subcellular localization and uptake of graphene quantum dots into solid tumors. Nanotechnology 2019, 30, 395101.

2. Hanahan, D.; Weinberg, R. Hallmarks of Cancer: The Next Generation. Cell 2011, 144, 646-674.

3. Siddik H. Zahid Mechanisms of Action of Cancer Chemotherapeutic Agents: DNA-Interactive Alkylating Agents and Antitumour Platinum-Based Drugs. 2002.

4. Thorn, C. F.; Oshiro, C.; Marsh, S.; Hernandez-Boussard, T.; McLeod, H.; Klein, T. E.; Altman, R. B. Doxorubicin pathways: pharmacodynamics and adverse effects. Pharmacogenet. Genomics 2011, 21, 440-446.

5. Riccio, A. A.; Schellenberg, M. J.; Williams, R. S. Molecular mechanisms of topoisomerase 2 DNA–protein crosslink resolution. Cellular and Molecular Life Sciences 2019.

6. Wallace, K.; Sardão, V.; Oliveira, P. Mitochondrial Determinants of Doxorubicin-Induced Cardiomyopathy. *Circulation Research* **2020***, 126*, 926-941.

7. Azzazy, H. M. E.; Mansour, M. M. H. In vitro diagnostic prospects of nanoparticles. *Clinica Chimica Acta* **2009***, 403*, 1-8.

8. Kah, J. C. Y.; Kho, K. W.; Lee, C. G. L.; James, C.; Sheppard, R.; Shen, Z. X.; Soo, K. C.; Olivo, M. C. Early diagnosis of oral cancer based on the surface plasmon resonance of gold nanoparticles. International journal of nanomedicine 2007, 2, 785-798.

9. Kushwaha, S. K. S.; Ghoshal, S.; Rai, A. K.; Singh, S. Carbon nanotubes as a novel drug delivery system for anticancer therapy: a review. Brazilian Journal of Pharmaceutical Sciences 2013, 49, 629-643.

10. Zhao, M.; Zhu, B. The Research and Applications of Quantum Dots as Nano-Carriers for Targeted Drug Delivery and Cancer Therapy. Nanoscale Res Lett 2016, 11, 1-9.

11. Teradal, N. L.; Jelinek, R. Carbon Nanomaterials in Biological Studies and Biomedicine. *Advanced Healthcare Materials* **2017***, 6*, 1700574-n/a.

12. Bahadar, H.; Maqbool, F.; Niaz, K.; Abdollahi, M. Toxicity of nanoparticles and an overview of current experimental models. *Iranian biomedical journal* **2016***, 20*, 1-11.

13. Dong, J.; Ma, Q. Type 2 Immune Mechanisms in Carbon Nanotube-Induced Lung Fibrosis. *Frontiers in immunology* **2018***, 9*, 1120.

14. Campbell, E.; Hasan, M. T.; Gonzalez Rodriguez, R.; Akkaraju, G. R.; Naumov, A. V. Doped Graphene Quantum Dots for Intracellular Multicolor Imaging and Cancer Detection. *ACS Biomaterials Science & Engineering* **2019***, 5*, 4671-4682.

15. Hafner, M.; Niepel, M.; Chung, M.; Sorger, P. K. Growth rate inhibition metrics correct for confounders in measuring sensitivity to cancer drugs. Nature methods 2016, 13, 521-527.

16. Harris, L. A.; Frick, P. L.; Garbett, S. P.; Hardeman, K. N.; Paudel, B. B.; Lopez, C. F.; Quaranta, V.; Tyson, D. R. An unbiased metric of antiproliferative drug effect in vitro. Nature methods 2016, 13, 497-500.